# Exoplanets

Xander Byrne

Michaelmas 2022

## 1 Detection

### 1.1 Transit

When a planet passes in front of a star, the total flux received from the star decreases by a factor of order $\Delta_0 \equiv R^2/R_*^2$. From detailed measurements of the light curve, one can also deduce $i$, $a/R_*$, and $P$. If the secondary eclipse is observed, one can also calculate $e$.

The transit method has been the most successful detection method, but it has drawbacks:

- For a transit to be observable, we require $i \approx 90°$, and hence large surveys are needed to find a good number of planets this way.
- The signal size is very small. $R_J/R_\odot = 0.100$, so $\Delta_{J,\odot} = 0.01$. Worse, $\Delta_{E,\odot} = 8.4 \times 10^{-5}$.
- To confirm the presence of a planet, multiple transits are required. This leads to long-period orbits being hard to detect with this method.

### 1.2 Radial Velocity

As a planet orbits a star, its star wobbles due to the gravitational pull of the planet on the star. The spectral lines in the star then oscillate with the radial velocity of the star. This oscillation will be sinusoidal for a circular orbit, but eccentricity distorts the RV curve. The whole system may have a systematic radial velocity, so the curve will generally be offset from $v_r = 0$. The *radial velocity semi-amplitude* $k$ of the curve depends on the parameters of the planet-star system. Assuming $M \gg M_*$:

$$k = \frac{1}{\sqrt{1-e^2}}\left(\frac{2\pi G}{PM_*^2}\right)^{1/3} M\sin i = \frac{0.0895\text{ms}^{-1}}{\sqrt{1-e^2}}\left(\frac{M\sin i}{M_E}\right)\left(\frac{M_*}{M_\odot}\right)^{-2/3}\left(\frac{P}{1\text{yr}}\right)^{-1/3}$$

Thus the signal size is largest for large planets around small stars on close-in, highly-inclined orbits. If the inclination is not independently known (such as through the transit method), then only $M\sin i$ can be deduced, giving a lower bound on $M$.

If the inclination is close enough to 90° that transit measurements can also be made, then it is possible to deduce $M$ and $R$. Hence the bulk density $\rho$ can be calculated, giving some clues as to its composition.

## 1.3 Direct Imaging

The viability of direct imaging depends on the *planet-star flux ratio* $F/F_*$, and separation $a$.

We first approximate both planet and star as black bodies. A black body has the specific intensity (see §2.1 later) given by the Planck law:

$$\boxed{B_\lambda = \frac{2hc^2}{\lambda^5}\frac{1}{e^{hc/\lambda k_B T}-1}} \xrightarrow{\lambda \gg hc/k_B T} \frac{2ck_BT}{\lambda^4}$$

where we have taken the large-wavelength limit $\lambda \gg hc/k_BT = 14\mu\text{m}/(T/1000\text{K})$; it is progressively easier to DI planets at longer wavelengths, as $F_\lambda/F_{*\lambda}$ is a monotonically-increasing function of $\lambda$, as is shown in Figure 1. This is intuitive, as the blackbody spectrum peaks according to Wien's law at $\lambda_{\max} = 2.9\text{mm K}/T$: a longer-wavelength peak for the cooler planet.

$$\frac{F_\lambda}{F_{*\lambda}} = \frac{B_\lambda(T)}{B_\lambda(T_*)}\frac{R^2}{R_*^2} = \frac{e^{hc/\lambda k_B T_*}-1}{e^{hc/\lambda k_B T}-1}\frac{R^2}{R_*^2} \xrightarrow{\lambda \gg hc/k_B T} \frac{T}{T_*}\frac{R^2}{R_*^2}$$

Figure 1 shows that the flux ratio between Jupiter and the Sun is only $\sim 10^{-4}$ even in the "far-infrared" ($\lambda > 15\mu$m); it is difficult to make ground-based measurements redwards of $5\mu$m due to FIR noise from the Earth.

The second issue is the separation. The angular separation is $\theta/\text{as} = (a/\text{AU})/(d/\text{pc})$. The diffraction limit of a telescope is $\theta/\text{rad} = 1.22\lambda/D$; for a 10m telescope in the visible, $\theta \sim 0.01$". However, most DI measurements are not diffraction-limited, but seeing-limited by Earth's atmospheric turbulence.

DI makes use of coronagraphy (to reduce the flux received from the star) and adaptive optics (to mitigate seeing) to improve the signal. Nonetheless, the best instruments have a flux sensitivity of $\sim 10^{-5}$ and an angular resolution of $\sim 0.2$" in the near-IR.

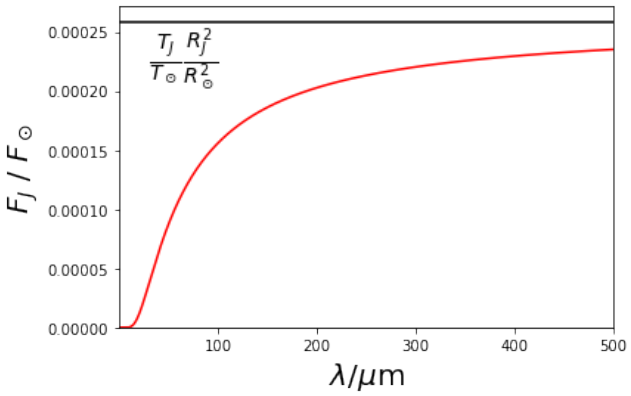


**Figure 1 | Planet-Star Flux Ratio between Jupiter and the Sun.** We have used $T_J = 150$K and $T_\odot = 5800$K, and $R_J/R_\odot = 0.1$. Note the large range of the horizontal axis

Note that all three detection methods are biased towards detecting large planets, whether in $M$ or $R$. RV is biased towards close-in planets whereas DI is biased towards far-out planets.

# 2 Atmospheres

## 2.1 Radiative Transfer

To understand how the composition and structure of an atmosphere can be deduced from observations, we must understand how light interacts with gases.

### 2.1.1 Specific Intensity and Flux

The specific intensity $I_\lambda$ is the amount of energy per unit wavelength passing through a unit area per unit time, distributed over a unit solid angle. As such, the energy travelling from an area $\mathrm{d}\mathbf{A}$ towards a solid angle $\mathrm{d}\Omega$ around the direction $\hat{\mathbf{n}}$ in a time $\mathrm{d}t$ is

$$\mathrm{d}E = I_\lambda \mathrm{d}\lambda\, \mathrm{d}\mathbf{A}\cdot\hat{\mathbf{n}}\mathrm{d}\Omega\, \mathrm{d}t = I_\lambda \mathrm{d}\lambda\, \mathrm{d}A\cos\theta\sin\theta \mathrm{d}\theta\mathrm{d}\phi\, \mathrm{d}t$$

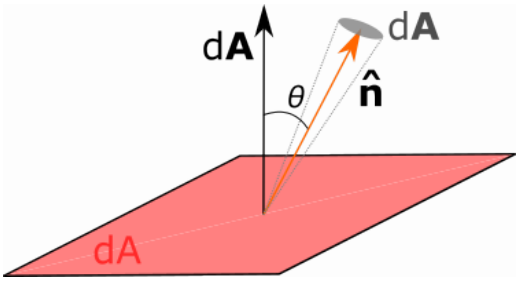


**Figure 2 | Specific Intensity**

Consider two surfaces $\mathrm{d}\mathbf{A}$ and $\mathrm{d}\mathbf{A}'$, separated by a distance $d$ in a direction $\hat{\mathbf{n}}$ to $\mathrm{d}\mathbf{A}$, and $\hat{\mathbf{n}}'$ to $\mathrm{d}\mathbf{A}'$. Let $\mathrm{d}\mathbf{A}$ emit light of a specific intensity $I_\lambda$ towards $\mathrm{d}\mathbf{A}'$; what specific intensity $I'_\lambda$ will the latter measure? The energy emitted by the former towards the latter is:

$$\mathrm{d}E = I_\lambda \mathrm{d}\lambda\, \mathrm{d}\mathbf{A}\cdot\hat{\mathbf{n}}\mathrm{d}\Omega\, \mathrm{d}t = I_\lambda \mathrm{d}\lambda [\mathrm{d}A\cos\theta]\left[\frac{\mathrm{d}A'\cos\theta'}{d^2}\right]\mathrm{d}t$$

where we have used $\mathrm{d}\Omega = \mathrm{d}A'\cos\theta'/d^2$. This must be equal to the energy received:

$$\mathrm{d}E = I'_\lambda\, \mathrm{d}\lambda\, \mathrm{d}\mathbf{A}'\cdot\hat{\mathbf{n}}'\mathrm{d}\Omega'\, \mathrm{d}t = I'_\lambda\, \mathrm{d}\lambda\, [\mathrm{d}A'\cos\theta']\left[\frac{\mathrm{d}A\cos\theta}{d^2}\right]\mathrm{d}t$$

Setting these two expressions equal, we find $I_\lambda = I'_\lambda$.

For a body whose $I_\lambda$ is isotropic outwards ($\theta < \pi/2$), but 0 inwards ($\theta > \pi/2$), the *specific flux* $F_\lambda$ (total energy in any direction per unit wavelength per unit time from a surface $\mathrm{d}\mathbf{A}$), is therefore:

$$F_\lambda \equiv \oint I_\lambda \cos\theta \mathrm{d}\Omega = I_\lambda \int_0^{2\pi}\int_0^{\pi/2} \cos\theta\sin\theta \mathrm{d}\theta\mathrm{d}\phi = \pi I_\lambda \quad \Rightarrow \quad \boxed{F_\lambda = \pi I_\lambda}$$

This is only true for the specific case that $I_\lambda$ is isotropic outwards, e.g. from the surface of a star. If $I_\lambda$ is known, then the *bolometric flux* $F$ can be derived by integrating over $\lambda$. E.g. for a black body, $I_\lambda = B_\lambda \Rightarrow F_\lambda = \pi B_\lambda$, so

$$F \equiv \int_0^\infty F_\lambda \mathrm{d}\lambda = \pi\int_0^\infty B_\lambda \mathrm{d}\lambda = 2\pi hc^2 \overbrace{\int_0^\infty \frac{1}{\lambda^5}\frac{\mathrm{d}\lambda}{e^{hc/\lambda k_B T}-1}}^{(\pi k_B T/hc)^4/15} = \overbrace{\frac{2\pi^5 k_B^4}{15h^3c^2}}^{\sigma} T^4 = \sigma T^4$$

the familiar Stefan-Boltzmann law. The total *power* from a black body is then $\int_\circ F\,\mathrm{d}A = 4\pi R_*^2 \sigma T^4$, and the flux then received at a distance $d$ is then $\sigma T^4 R_*^2/d^2$, as is familiar.

### 2.1.2 Moments of Specific Intensity

If $I_\lambda$ is not isotropic, but is rather axisymmetric about the surface normal (i.e. angular dependence only on $\mu = \cos\theta$), we can define the *mean specific intensity* $J_\lambda$:

$$J_\lambda \equiv \frac{1}{4\pi}\int_0^{2\pi} \mathrm{d}\phi \int_0^{\pi} I_\lambda(\theta)\sin\theta \mathrm{d}\theta = \frac{1}{2}\int_{-1}^{1} I_\lambda(\mu)\mathrm{d}\mu$$

where we now allow $\theta \in [0, \pi]$ so that some $I_\lambda$ might be directed inwards. We extend this definition to the $n$th *moment* of the specific intensity:

$$M_\lambda^n \equiv \frac{1}{2}\int_{-1}^{1} \mu^n I_\lambda(\mu)\mathrm{d}\mu \qquad \Rightarrow \qquad J_\lambda \equiv M_\lambda^0; \qquad H_\lambda \equiv M_\lambda^1 \equiv \frac{1}{2}\int_0^{\pi} I_\lambda(\theta)\cos\theta\sin\theta\mathrm{d}\theta$$

Note that the *Eddington flux* $H_\lambda = F_\lambda/4\pi$, where $F_\lambda = \int_0^{2\pi}\int_0^{\pi} I_\lambda \cos\theta\sin\theta \mathrm{d}\phi$. The second moment $M_\lambda^2 \equiv K_\lambda$ is called the *K-integral*, and is related to radiation pressure.

### 2.1.3 Absorption, Scattering, and Emission

When light of specific intensity $I_\lambda$ passes through a volume of gas of thickness $\mathrm{d}s$ and cross-sectional area $\mathrm{d}A$, the specific intensity changes by $\mathrm{d}I_\lambda$. This change is due to three processes, all of which impart a $\mathrm{d}I_\lambda$ proportional to the mass of gas in the volume, $\rho\,\mathrm{d}A\,\mathrm{d}s$:

- **Absorption.** The amount of incident light absorbed and dissipated into internal energy:

  $$\mathrm{d}E_{\lambda,\mathrm{a}} = -\kappa_\lambda \rho I_\lambda\,\mathrm{d}A\,\mathrm{d}s\,\mathrm{d}\Omega\mathrm{d}\lambda\,\mathrm{d}t$$

  where the *absorption coefficient* $\kappa_\lambda$ has units of $\mathrm{cm}^2\mathrm{g}^{-1}$, and depends on composition.

- **Scattering.** The fraction of incident light diverted from the incident direction. $I_\lambda$ refers to a particular direction; the amount of light heading in that direction is reduced by being scattered away, but increased by light in *other* directions being scattered into the direction of interest. The out-scattering is proportional to the incident intensity, whereas the in-scattering is proportional to the mean intensity over all directions. Therefore

  $$\mathrm{d}E_{\lambda,\mathrm{s}} = (-\sigma_\lambda I_\lambda + \sigma_\lambda J_\lambda)\rho\,\mathrm{d}A\,\mathrm{d}s\,\mathrm{d}\Omega\mathrm{d}\lambda\,\mathrm{d}t$$

  where the *scattering coefficient* $\sigma_\lambda$ has the same units as $\kappa_\lambda$, $\mathrm{cm}^2\mathrm{g}^{-1}$.

- **Emission.** The thermal emission of the gas. Importantly, emission is independent of $I_\lambda$.

  $$\mathrm{d}E_{\lambda,e} = +j_\lambda^t \rho\,\mathrm{d}A\,\mathrm{d}s\,\mathrm{d}\Omega\mathrm{d}\lambda\,\mathrm{d}t$$

  In *local thermodynamic equilibrium* (locally homogeneous $T$, in thermodynamic equilibrium with radiation field, behaves as a black body), the energy emitted is equal to the energy absorbed by a black body, in which case the *thermal emissivity* $j_\lambda^t = \kappa_\lambda B_\lambda(T)$.

The change in specific intensity is therefore given by

$$\mathrm{d}I_\lambda = \frac{\mathrm{d}E_{\lambda,\mathrm{a}} + \mathrm{d}E_{\lambda,\mathrm{s}} + \mathrm{d}E_{\lambda,\mathrm{e}}}{\mathrm{d}\lambda\,\mathrm{d}A\,\mathrm{d}\Omega\,\mathrm{d}t} = \big(\overbrace{\kappa_\lambda B_\lambda + \sigma_\lambda J_\lambda}^{j_\lambda} \overbrace{-\sigma_\lambda I_\lambda - \kappa_\lambda I_\lambda}^{-k_\lambda I_\lambda}\big)\rho\,\mathrm{d}s$$

$$\Rightarrow \boxed{\frac{1}{\rho}\frac{\mathrm{d}I_\lambda}{\mathrm{d}s} = j_\lambda - k_\lambda I_\lambda} \qquad (\mathfrak{RTE})$$

where $j_\lambda$, due to both thermal emission and out-scattering, is called just the *emissivity* and $k_\lambda = \kappa_\lambda + \sigma_\lambda$ the overall *extinction coefficient*. The above result is called the *radiative transfer equation*. It can be alternatively expressed as

$$\boxed{\frac{1}{k_\lambda \rho}\frac{\mathrm{d}I_\lambda}{\mathrm{d}s} = S_\lambda - I_\lambda} \qquad \text{where} \qquad S_\lambda \equiv \frac{j_\lambda}{k_\lambda} = \frac{\kappa_\lambda B_\lambda + \sigma_\lambda J_\lambda}{\kappa_\lambda + \sigma_\lambda}$$

where we have defined the *source function* $S_\lambda$. If $\kappa_\lambda \gg \sigma_\lambda$, which we describe as *glossy*[1], $k_\lambda \approx \kappa_\lambda$ and $S_\lambda \approx B_\lambda$. I have no idea how realistic that is: I can't find any values for $\kappa_\lambda$ or $\sigma_\lambda$.

## 2.2 Temperature Profiles

The temperature structure of an atmosphere is due to the energy transport processes occurring therein: **radiation** and **convection**.

### 2.2.1 Radiative Equilibrium

*Radiative equilibrium* is a state where the thermal energy leaving a body is equal to that absorbed. The temperature structure can then be found from balancing inputs and outputs of radiative energy. Assuming no external sources, the *total flux per unit mass* $f$ that is *emitted* into the radiation field by a portion of the atmosphere is, recalling that $j_\lambda$ is isotropic,

$$f_e = \int_0^\infty \mathrm{d}\lambda \oint \mathrm{d}\Omega\ j_\lambda = 4\pi \int_0^\infty k_\lambda S_\lambda \mathrm{d}\lambda = 4\pi \int_0^\infty (\kappa_\lambda B_\lambda + \sigma_\lambda J_\lambda)\mathrm{d}\lambda$$

The total flux/mass which is *absorbed* from the radiation field is, recalling the definition of $J_\lambda$,

$$f_a = \int_0^\infty \mathrm{d}\lambda \oint \mathrm{d}\Omega\ k_\lambda I_\lambda = 4\pi \int_0^\infty k_\lambda J_\lambda \mathrm{d}\lambda = 4\pi \int_0^\infty (\kappa_\lambda J_\lambda + \sigma_\lambda J_\lambda)\mathrm{d}\lambda$$

Setting these equal, we obtain $\boxed{\int_0^\infty k_\lambda (J_\lambda - S_\lambda)\mathrm{d}\lambda = \int_0^\infty \kappa_\lambda (J_\lambda - B_\lambda)\mathrm{d}\lambda = 0}$. This is true at any location in the atmosphere in radiative equilibrium. The $T$ structure (represented by $B_\lambda$) and the radiation field (represented by $J_\lambda$) are thus intrinsically linked.

### 2.2.2 Isolated, Glossy, Grey Atmospheres

$\mathfrak{RTE}$ can be written: $$\frac{\mu}{k_\lambda \rho}\frac{\mathrm{d}I_\lambda}{\mathrm{d}z} = S_\lambda - I_\lambda$$

where we have introduced $\mu = \mathrm{d}z\,/\,\mathrm{d}s$, where $z$ is atmospheric altitude. Integrating over solid angle and recalling that $H_\lambda$ is the first moment of $I_\lambda$, we have $\frac{1}{k_\lambda \rho}\frac{\mathrm{d}H_\lambda}{\mathrm{d}z} = S_\lambda - J_\lambda$. Recalling also that $H_\lambda = F_\lambda / 4\pi$, and that the total flux $F = \int F_\lambda \mathrm{d}\lambda$, the quantity $\mathrm{d}F/\mathrm{d}z$ is given by:

$$\frac{\mathrm{d}F}{\mathrm{d}z} = \frac{\mathrm{d}}{\mathrm{d}z}\int_0^\infty F_\lambda \mathrm{d}\lambda = 4\pi \frac{\mathrm{d}}{\mathrm{d}z}\int_0^\infty H_\lambda \mathrm{d}\lambda = 4\pi \int_0^\infty \frac{\mathrm{d}H_\lambda}{\mathrm{d}z}\mathrm{d}\lambda = 4\pi\rho \underbrace{\int_0^\infty k_\lambda (S_\lambda - J_\lambda)\mathrm{d}\lambda}_{0} = 0$$

[1] There doesn't seem to be a specific adjective for "in the absence of scattering", so I've gone with "glossy", as that's what solid surfaces look like without scattering.

Thus the total flux $F$ is constant in height, for an atmosphere in radiative equilibrium (i.e. not currently heating up or cooling down due to the radiation field).

Consider the *first moment* of $\mathfrak{RTE}$. Multiplying by $\mu$ and integrating over $\mathrm{d}\Omega$, we find $\frac{\mathrm{d}K_\lambda}{\mathrm{d}z} = k_\lambda \rho H_\lambda$, where we recall that $K_\lambda$ is the *second* moment of $I_\lambda$; the integral $\oint \mu S_\lambda \mathrm{d}\Omega = 0$, because $S_\lambda$ (being a linear combination of the isotropic $B_\lambda$ and $J_\lambda$) is isotropic. Under the *Eddington approximation*, which assumes a linear form for $I_\lambda(\mu) = I^0_\lambda + I^1_\lambda \mu$, we find

$$K_\lambda = \frac{1}{2}\int_{-1}^{1} \left(I^0_\lambda + I^1_\lambda \mu\right)\mu^2 \mathrm{d}\mu = \frac{I^0_\lambda}{3}; \qquad J_\lambda = \frac{1}{2}\int_{-1}^{1} \left(I^0_\lambda + I^1_\lambda \mu\right)\mathrm{d}\mu = I^0_\lambda \qquad \Rightarrow \qquad K_\lambda = \frac{J_\lambda}{3}$$

and recalling that $H_\lambda = F_\lambda / 4\pi$, we obtain

$$\frac{\mathrm{d}J_\lambda}{\mathrm{d}z} = 3\frac{\mathrm{d}K_\lambda}{\mathrm{d}z} = 3k_\lambda \rho H_\lambda = \frac{3k_\lambda \rho F_\lambda}{4\pi}$$

We now consider a *glossy grey* atmosphere, where $k_\lambda = \kappa_\lambda = \bar{\kappa} \forall \lambda$. Under this approximation, the opacity can be taken outside of the radiative equilibrium integral above and we have $J \equiv \int J_\lambda \mathrm{d}\lambda = \int B_\lambda \mathrm{d}\lambda = \sigma T^4 / \pi$. Integrating the previous expression for $\mathrm{d}J_\lambda/\mathrm{d}z$ over $\mathrm{d}\lambda$, and writing the constant flux $F \equiv \int F_\lambda \mathrm{d}\lambda = \sigma T^4_{\mathrm{eff}}$ for some *effective temperature* $T_{\mathrm{eff}}$,

$$\frac{\mathrm{d}}{\mathrm{d}z}\frac{\sigma T^4}{\pi} = -\frac{3\bar{\kappa}\rho}{4\pi}F \qquad \Rightarrow \qquad \frac{\mathrm{d}T^4}{\mathrm{d}z} = -\frac{3\bar{\kappa}\rho}{4}T^4_{\mathrm{eff}}$$

giving an ODE for the temperature structure in an isolated atmosphere. We see that $T$ monotonically decreases with height.

We can't integrate this straight away to obtain $T(z)$ because $\bar{\kappa}$ and $\rho$ may change with $z$. We instead define the *optical depth* $\tau_\lambda$: $\mathrm{d}\tau_\lambda = -k_\lambda \rho \, \mathrm{d}z$; in this case $\mathrm{d}\tau_\lambda = \mathrm{d}\tau = -\bar{\kappa}\rho \, \mathrm{d}z \, \forall \lambda$. The optical depth is a dimensionless property of a path which quantifies how "difficult" it is for light to travel that path: higher $k_\lambda$ and higher $\rho$ encourage large negative $\mathrm{d}I_\lambda$. As $\mathrm{d}\tau_\lambda \propto -\mathrm{d}z$, deeper layers in the atmosphere have a *larger* optical depth. Changing variables $z \to \tau$,

$$\frac{\mathrm{d}T^4}{\mathrm{d}\tau} = \frac{3}{4}T^4_{\mathrm{eff}} \qquad \Rightarrow \qquad T^4 = \frac{3}{4}T^4_{\mathrm{eff}}\left(\tau + \frac{2}{3}\right)$$

where the integration constant comes from the boundary condition that $T = T_{\mathrm{eff}}$ at $\tau = 2/3$, which is often taken to be the conventional "outer edge" of a black body. As $\tau \to 0$ (that is, the top of the atmosphere), $T \to 2^{-1/4} T_{\mathrm{eff}} \approx 0.84 T_{\mathrm{eff}}$ (the "skin temperature" of the body); the $T$ profile thus tends to an isotherm at high altitudes.

### 2.2.3 Irradiated Atmospheres

An analysis by Guillot (2010) found the following profile for an irradiated atmosphere:

$$T^4 = \frac{3}{4}T^4_{\mathrm{int}}\left(\tau + \frac{2}{3}\right) + \frac{3}{4}T^4_{\mathrm{irr}} f \left[\frac{2}{3} + \frac{1}{\gamma\sqrt{3}} + \left(\frac{\gamma}{\sqrt{3}} - \frac{1}{\gamma\sqrt{3}}\right)e^{-\gamma\tau/\sqrt{3}}\right]$$

where (deep breath) $\sigma T^4_{\mathrm{int}}$ is the flux emitted by the planet (the same role as $T_{\mathrm{eff}}$ in the isolated case), $\sigma T^4_{\mathrm{irr}} \equiv \sigma T^4_* R^2_* / a^2$ is the flux received at the top of the atmosphere from the external source, $f$ is an *Eddington coefficient* accounting for the *redistribution* of the incident energy[2], and $\gamma \equiv \bar{\kappa}_{\mathrm{vis}} / \bar{\kappa}_{\mathrm{th}}$ is the ratio of the mean opacity in the UV/visible to that in the IR.

[2] At the substellar point, $f = 1$; for a dayside average, $f = 1/2$; for a planetary average, $f = 1/4$

If $T_{\rm irr} \ll T_{\rm int}$, we naturally recover the isolated case (above). Thus we henceforth consider the case $T_{\rm irr} \gg T_{\rm int}$, as is the case for Hot Jupiters; the full profiles will be somewhere in between. For small $\tau \approx 0$, $T$ tends to a constant:

$$T(\tau = 0) = T_{\rm irr}\left[\frac{3}{4}f\left(\frac{2}{3} + \frac{\gamma}{\sqrt{3}}\right)\right]^{1/4}$$

so as in the isolated case, the profile tends to an isotherm at high altitude – though now of order $T_{\rm irr}$, which may be 1000s of K, whereas $T_{\rm int} \sim 10^2$K. For larger $\tau$, consider the derivative:

$$\frac{{\rm d}T^4}{{\rm d}\tau} = \frac{3}{4}T_{\rm int}^4 + \frac{1}{4}T_{\rm irr}^4 f\left(1-\gamma^2\right)e^{-\gamma\tau/\sqrt{3}} \approx \frac{1}{4}T_{\rm irr}^4 f\left(1-\gamma^2\right)e^{-\gamma\tau/\sqrt{3}}$$

The sign thus depends on the sign of $1-\gamma^2$. If $\gamma > 1$, that is, the UV/vis opacity is higher than the thermal opacity, then ${\rm d}T/{\rm d}\tau < 0$: a *thermal inversion* occurs, where the temperature *rises* with altitude. Thermal inversions are therefore induced by species with high $\bar{\kappa}_{\rm vis}$, such as $O_3$ (as on Earth), TiO, VO, or photochemical hazes (as is the case on Jupiter).

For $\tau \gg 1$, ${\rm d}T^4/{\rm d}\tau = 3T_{\rm int}^4/4$, so the derivative ${\rm d}(T/T_{\rm int})/{\rm d}\tau \sim T_{\rm int}^3/T^3 \ll 1$. The profile thus tends to an isotherm again. Very deep in the atmosphere, the density is so high that radiative energy transport is less efficient than convection, and the profile will tend to an adiabat (see §2.2.5). This occurs at $\lesssim 10^4$bar.

### 2.2.4 Atmospheric Retrievals

Atmospheres are complicated. To properly model them, one must solve self-consistently for the temperature profile, the radiation field, the chemical composition at different altitudes, the presence of clouds & hazes etc., which requires a lot of computing time. However, most atmospheric temperature profiles can be accurately approximated by models with rather small numbers of parameters. One can similarly parametrise the effects of other properties of the atmosphere, such as composition.

If one is trying to infer atmospheric properties from a spectrum, one therefore need not compare it to spectra of accurate, polished model atmospheres found off the shelf. One can *fit* it to a spectrum from a space of rough, not-quite-self-consistent-but-parametrised atmospheric models, finding the parameters which best fit the spectrum. Restricting the model to this approximate parametrised form greatly reduces the computating time. This process is called *atmospheric retrieval*.

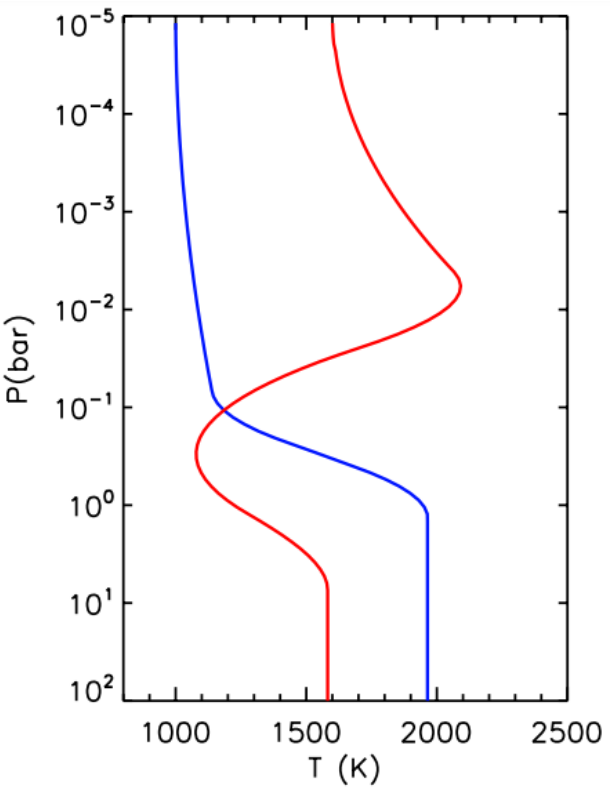


**Figure 3 | Temperature Profiles of Irradiated Atmospheres.** Stolen from Madhusudhan & Seager (2010). At both high and low altitudes, the profiles tends to an isotherm. Depending on the atmospheric composition, there may or may not be a temperature inversion in the middle. These profiles do not show the effects of convection, which cause the profile to tend to an adiabat below $p \sim 10^4$bar.

### 2.2.5 Convection

Consider a parcel of gas, initially of the same $\rho$ and $T$ of the surrounding atmosphere. Suppose it is perturbed such that it rises adiabatically, and therefore maintains pressure equilibrium with the surroundings. $\rho T \propto p$ is therefore always matched between the parcel and the surroundings. Now if the atmosphere is stable to convection, once risen the parcel will sink back down, meaning it must have become denser, and therefore cooler, than its new surroundings: the parcel must cool down *faster* than the surroundings as it rises. By contrast, if the atmosphere is *unstable* to convection, the parcel will become *less* dense than its new surroundings, and thus *hotter*: the parcel must cool down *slower* than the surroundings. Thus

$$\text{Stable:} \quad \left.\frac{\mathrm{d}T}{\mathrm{d}z}\right|_{\text{parcel}} < \left.\frac{\mathrm{d}T}{\mathrm{d}z}\right|_{\text{surr.}} \qquad \text{Unstable:} \quad \left.\frac{\mathrm{d}T}{\mathrm{d}z}\right|_{\text{parcel}} > \left.\frac{\mathrm{d}T}{\mathrm{d}z}\right|_{\text{surr.}}$$

Look at it again to make sure you get which way round it is.

What is the critical temperature gradient to decide if an atmosphere is stable or unstable to convection? It is the temperature gradient *equal* to that of an adiabatically rising parcel of gas. For such a parcel $p \propto \rho^\gamma$ and $p \propto \rho T$, so

$$\frac{\mathrm{d}p}{p} = \gamma\frac{\mathrm{d}\rho}{\rho}, \qquad \frac{\mathrm{d}p}{p} = \frac{\mathrm{d}\rho}{\rho} + \frac{\mathrm{d}T}{T} \qquad \Rightarrow \qquad \frac{\mathrm{d}T}{T} = \left(1 - \frac{1}{\gamma}\right)\frac{\mathrm{d}p}{p}$$

$$\Rightarrow \left.\frac{\mathrm{d}T}{\mathrm{d}z}\right|_{\text{parcel}} = \frac{\gamma-1}{\gamma}\frac{T}{p}\frac{\mathrm{d}p}{\mathrm{d}z} = -\frac{\gamma-1}{\gamma}\frac{\mu}{k_B}g \equiv -\frac{g}{c_P}$$

where we have used hydrostatic equilibrium ($\mathrm{d}p/\mathrm{d}z = -\rho g$), and the definition of the specific heat capacity $c_P$ (per unit mass, units $\mathrm{JK^{-1}kg^{-1}}$). If the atmosphere's temperature gradient is less than this value (which is negative – so a *steeper* negative gradient), then the atmosphere's temperature will fall away from the parcel's, the parcel will be buoyant, and the atmosphere will be unstable to convection. This sets a minimum temperature gradient – if the gradient is ever too negative then convection will activate and bring the profile up onto an adiabat.

Note that regions of temperature inversion ($\mathrm{d}T/\mathrm{d}z > 0$) are always stable to convection. Gas parcels rise, cool somewhat to maintain pressure equilibrium, but find themselves amongst hotter gas and sink back down.

Recall that for an isolated atmosphere, $\mathrm{d}T^4/\mathrm{d}z = -3\bar{\kappa}\rho T_{\text{eff}}^4/4 \propto -\rho$. In the lower atmosphere, where the density is highest (and where the influence of irradiation is reduced so that the atmosphere can be approximated as isolated), the temperature gradient due to radiative energy transport is most negative, and so most unstable to convection. Convection therefore dominates the energy transport at low altitudes, and the temperature profile follows an adiabat. Higher in the atmosphere, radiation becomes an efficient transport mechanism due to the lower density, so the temperature gradient becomes less steep and the atmosphere is stable to convection. The atmosphere switches modes at the altitude where $\mathrm{d}T/\mathrm{d}z\,\big|_{\text{rad.}}$ is equal to the adiabatic value, typically where $p \sim 10^4$bar. Assuming stellar irradiation is negligible at this depth, we can write this equality as:

$$-\frac{3\bar{\kappa}\rho}{16\sigma T^3}F = -\frac{g}{c_P} \qquad \Rightarrow \qquad \frac{\rho}{T^3} = \frac{16\sigma g}{3\bar{\kappa}c_P F} \qquad \Rightarrow \qquad \rho_{\text{rc}} \propto T^3 \qquad \Rightarrow \qquad p_{\text{rc}} \propto T^4$$

Thus on hotter planets, we expect to have to go deeper to see convection take over.

## 2.3 Emission Spectra

Direct imaging, by default, measures the planet's *emission spectrum*. This spectrum will mostly be the black-body-ish thermal spectrum of the planet (likely peaking in the NIR). Many planets additionally have a large *albedo* $A$ (see §2.6.2), reflecting the light of the star. As such, superposed onto the *planetary* thermal spectrum will be a small amount of the *stellar* thermal spectrum, peaking in the UV/visible – the overall emission spectrum should therefore be double-peaked. However, stars being very bright at these wavelengths is the whole reason that DI measurements are not made in the UV/visible. We therefore consider just the planetary thermal emission.

We have from §2.1 that $\frac{1}{k_\lambda \rho}\frac{\mathrm{d}I_\lambda}{\mathrm{d}s} = -\mu\frac{\mathrm{d}I_\lambda}{\mathrm{d}\tau_\lambda} = S_\lambda - I_\lambda$. Integrating from $\tau_1$ to $\tau_2 < \tau_1$ (upwards),

$$\mu\frac{\mathrm{d}}{\mathrm{d}\tau_\lambda}\left(I_\lambda e^{-\tau_\lambda/\mu}\right) = -S_\lambda e^{-\tau_\lambda/\mu} \quad \Rightarrow \quad \mu\left(I_\lambda(\tau_2)e^{-\tau_2/\mu} - I_\lambda(\tau_1)e^{-\tau_1/\mu}\right) = -\int_{\tau_1}^{\tau_2} S_\lambda(\tau)e^{-\tau/\mu}\mathrm{d}\tau$$

$$\Rightarrow I_\lambda(\tau_2) = I_\lambda(\tau_1)e^{-(\tau_1-\tau_2)/\mu} + \frac{e^{\tau_2/\mu}}{\mu}\int_{\tau_2}^{\tau_1} S_\lambda(\tau)e^{-\tau/\mu}\mathrm{d}\tau$$

where we leave implicit the $\lambda$-dependence of $\tau$ for to avoid subscripts.

### 2.3.1 Isothermal Glossy Atmospheres

The simplest model of an atmosphere is an isothermal one, at $T$. The pressure is such that

$$\frac{\mathrm{d}p}{\mathrm{d}z} = -\rho g = -\frac{\mu g}{k_B T}p \qquad \Rightarrow \qquad p(z) = p_0 \exp\left(-\frac{z}{H_{\mathrm{sc}}}\right) \qquad \boxed{H_{\mathrm{sc}} = \frac{k_B T}{\mu g}}$$

where we define the *scale height* $H_{\mathrm{sc}}$. Earth's scale height is about 9km.

For an isothermal glossy atmosphere, $S_\lambda = B_\lambda$ and $B_\lambda$ is independent of $\tau_\lambda$, as $B_\lambda$'s only path-dependence is on the temperature which we assume constant. Thus,

$$I_\lambda(\tau_2) = I_\lambda(\tau_1)e^{-(\tau_1-\tau_2)/\mu} + \frac{e^{\tau_2/\mu}}{\mu}B_\lambda\int_{\tau_2}^{\tau_1} e^{-\tau/\mu}\mathrm{d}\tau = I_\lambda(\tau_1)e^{-(\tau_1-\tau_2)/\mu} + B_\lambda\left(1 - e^{-(\tau_1-\tau_2)/\mu}\right)$$

Consider a *semi-infinite atmosphere*, where the radiation originates in the depths of the atmosphere where $\tau_1 \to \infty$; we observe at $\tau_2 = 0$. The factor $e^{-(\tau_1-\tau_2)} = 0$. The specific intensity we observe is then $I_\lambda(\tau{=}0) = B_\lambda$, independent of composition. Therefore, *the emission spectrum of an isothermal atmosphere is a black body spectrum.*

### 2.3.2 Effect of Temperature Structure

Consider a thin glossy layer of an atmosphere, of optical thickness $\Delta\tau_\lambda \ll 1$, between $\tau_\lambda = \tau_1$ and $\tau_\lambda = \tau_2$. The thin layer is at constant temperature, so we can evaluate the integral as above. Now $\tau_1 - \tau_2 = \Delta\tau_\lambda \ll 1$, so $e^{-(\tau_1-\tau_2)/\mu} \approx 1 - \Delta\tau_\lambda/\mu$, and we have

$$I_\lambda(\tau_2) \approx I_\lambda(\tau_1)(1 - \Delta\tau_\lambda/\mu) + B_\lambda\Delta\tau_\lambda/\mu \qquad \Rightarrow \qquad I_\lambda(\tau_2) - I_\lambda(\tau_1) = \Delta\tau_\lambda(B_\lambda - I_\lambda(\tau_1))/\mu$$

From this we can make the following conclusions:

- If $B_\lambda < I_\lambda(\tau_1)$ (i.e. the layer we are considering is *cooler* than the layer below, represented by $I_\lambda(\tau_1)$), then $I_\lambda(\tau_2) < I_\lambda(\tau_1)$: an *absorption* feature is observed.

- If $B_\lambda > I_\lambda(\tau_1)$ (i.e. the layer we are considering is *hotter* than the layer below: a *temperature inversion*), then $I_\lambda(\tau_2) > I_\lambda(\tau_1)$: an *emission* feature is observed, and the spectrum exceeds the black body curve.
- If $\Delta\tau_\lambda = 0$, for example if we are looking at a wavelength at which the atmosphere is transparent, $I_\lambda(\tau_2) = I_\lambda(\tau_1)$. Extrapolating down, the spectrum will simply be that emitted from the surface: a black body.

We see that for the spectrum to deviate from a black-body spectrum, we require both absorbing species *and* temperature variation. For example, for a monotonically-decreasing temperature profile, the spectrum is a black-body spectrum with bites taken out of it at wavelengths which are absorbed by species present in the atmosphere. Conversely if $I_\lambda$ never exceeds the black-body curve[3], then the atmosphere must have a monotonically-decreasing $T$ profile.

## 2.4 Transmission Spectra

### 2.4.1 Primary Transit

From §1.1, we have $\Delta_0 \equiv R^2/R_*^2$, but this was for an opaque sphere. Due to the atmosphere, $\Delta$ is wavelength-dependent. For an atmosphere of wavelength-dependent "height" $h_\lambda$, we have

$$\Delta_\lambda = \left(\frac{R + h_\lambda}{R_*}\right)^2 \approx \Delta_0 + \frac{2h_\lambda R}{R_*^2} \equiv \Delta_0 + \delta_\lambda \qquad \Rightarrow \qquad \boxed{\delta_\lambda = \frac{2h_\lambda R}{R_*^2}}$$

where we have neglected terms of order $h^2/R_*^2$. Note that the additional $\delta_\lambda = 2\pi R h_\lambda/\pi R_*^2$, the area of an annulus of radius $R$ and thickness $h_\lambda \ll R$ divided by the area of the stellar disk, intuitively. $h_\lambda$ depends on the composition and structure of the atmosphere, so by recording a *transmission spectrum* (that is to say, measuring the function $h_\lambda$), these can be estimated. $h_\lambda$ is typically bounded between 5 and 8 scale heights $H_{\text{sc}}$.

### 2.4.2 Radiative Transfer Model

Consider a plane-parallel slab of gas, and some radiation from a hot star passing through. Where the temperature of the gas is much colder than that of the radiation, the gas is not going to be emitting much energy compared to that going through it, and so the atmosphere's effect will simply be to absorb. We therefore have $S_\lambda \ll I_\lambda$, and $\mathrm{d}I_\lambda/\mathrm{d}s = -k_\lambda \rho I_\lambda$. Writing $\mathrm{d}\tau_\lambda = k_\lambda \rho \,\mathrm{d}s$ (we are now simply considering light passing through some gas at normal incidence, not looking down into an atmosphere), we then have

$$\frac{\mathrm{d}I_\lambda}{\mathrm{d}\tau_\lambda} = -I_\lambda \qquad \Rightarrow \qquad I_\lambda(\tau_\lambda) = I_\lambda(0)e^{-\tau_\lambda} \qquad \text{(Beer-Lambert Law)}$$

The flux received (at Earth) from the star out of transit is $F_{*\lambda} = \pi I_{\lambda *} R_*^2/d^2$. In transit, we deduce the flux received at Earth $F_{t\lambda}$ by integrating over annuli of solid angle $2\pi r\,\mathrm{d}r\,/d^2$, including the atmospheric height $h_\lambda$:

$$F_{t\lambda} = \int_0^R I_\lambda \frac{2\pi r\,\mathrm{d}r}{d^2} + \int_R^{R+h_\lambda} I_{\lambda *} e^{-\tau_\lambda(r)} \frac{2\pi r\,\mathrm{d}r}{d^2} + \int_{R+h_\lambda}^{R_*} I_{\lambda *} \frac{2\pi r\,\mathrm{d}r}{d^2}$$

[3]The temperature of black-body curve to use as a "baseline" is found by looking at a wavelength where it is known that the atmosphere is transparent and $\tau_\lambda = 0$.

Approximating the atmosphere as cylindrical (such that $\tau_\lambda$ is independent of $r$), this is

$$F_{t\lambda} = \frac{\pi}{d^2}\left[I_\lambda R^2 + I_{\lambda *}\left[e^{-\tau_\lambda}\left((R+h_\lambda)^2 - R^2\right) + R_*^2 - (R+h_\lambda)^2\right]\right]$$

The flux ratio $\Delta_\lambda \equiv (F_{*\lambda} - F_{t\lambda})/F_{*\lambda}$ is then given by

$$\begin{aligned}\Delta_\lambda &= 1 - \frac{1}{R_*^2}\left[\underbrace{\frac{I_\lambda}{I_{\lambda *}}R^2}_{\ll R^2} + e^{-\tau_\lambda}\underbrace{\left(2Rh_\lambda + h_\lambda^2\right)}_{\approx 2Rh_\lambda} + R_*^2 - \underbrace{(R+h_\lambda)^2}_{\approx R^2 + 2Rh_\lambda}\right] \approx \frac{R^2 + 2Rh_\lambda(1-e^{-\tau_\lambda})}{R_*^2} \\ &= \Delta_0 + \frac{2Rh_\lambda}{R_*^2}\left(1 - e^{-\tau_\lambda}\right)\end{aligned}$$

We see that $\delta_\lambda$ has been modified by a factor $1 - e^{-\tau_\lambda}$. In the limit of $\tau_\lambda \to 0$ (a transparent atmosphere), this factor tends to 0 and $\Delta_\lambda \to \Delta_0$. In the limit of $\tau_\lambda \to \infty$ (an opaque atmosphere), this factor tends to 1 and $\delta_\lambda$ takes its previous value. $h_\lambda$ depends on composition, and $\tau_\lambda$ definitely does as it relates to $k_\lambda$.

### 2.4.3 Secondary Eclipse

Just before the planet is occulted by the star, the flux received is from both the planet and the star $F_\lambda + F_{*\lambda}$; after occultation we only see the stellar flux $F_{*\lambda}$. The signal size is the fractional flux drop, equal to $F_\lambda/F_{*\lambda}$. This depends on wavelength as discussed in §1.3; the flux ratio plateau reveals the planet's temperature compared to the star's.

## 2.5 Chemical Composition

Crucial to the radiative properties of the atmosphere, and hence the observed emission and transmission spectra, is the extinction coefficient $k_\lambda = \kappa_\lambda + \sigma_\lambda$. The wavelength dependence of $k_\lambda$ ultimately depends on the *composition* of the atmosphere.

### 2.5.1 Equilibrium Chemistry

A box of gas of a given elemental composition, temperature, and pressure has a unique set of abundances of all chemical species, once allowed to settle to chemical equilibrium. Some noble elements will stay in atomic form, but most will form molecules.

Consider a portion of gas, connected to another large reservoir of gas (e.g. some gas connected to the atmosphere) such that any temperature or pressure changes due to chemical reactions are quickly erased. The first law of thermodynamics gives $\mathrm{d}U = \delta Q + \delta W$. The Gibbs free energy is defined as $G = U + pV - TS$, so its differential is

$$\mathrm{d}G = \mathrm{d}U + p\,\mathrm{d}V + V\underbrace{\mathrm{d}p}_{0} - T\,\mathrm{d}S - S\underbrace{\mathrm{d}T}_{0} = \underbrace{\delta Q - T\,\mathrm{d}S}_{\leq 0 \;\because\; 2\mathfrak{LT}} + \underbrace{\delta W + p\,\mathrm{d}V}_{0} \leq 0$$

Thus chemical reactions taking place at constant $T$ and $p$ cause a reduction in $G$. At chemical equilibrium, by definition no net reactions occur and $\mathrm{d}G = 0$. Thus to find the equilibrium chemical composition of some gas of a given elemental composition, $T$, and $p$, we must find the chemical composition that minimises the total $G$ of the mixture. To do this, we must consider the $G_i$ of the individual species involved.

Although we are taking the overall $p$ as fixed, the *partial pressures* $\{p_i\}$ depend on how much of each species there is. $p_i$ is what the overall pressure *would* be if species $i$ were the only thing there. Ideal gases do not have intermolecular interactions, so the presence of another species $j$ does not affect the partial pressure of species $i$. The total pressure is therefore the sum of all the partial pressures. Ideal gases have $p = nRT/V$, so $p_i/p_{\rm tot} = n_i/n_{\rm tot}$ (this quantity is known as the *volume mixing ratio* for some reason). Thus whereas the temperature is fixed for a given species, its *pressure* depends on the composition, so when we are minimising $G_{\rm tot}$, we need to find the right abundance (and hence $n_i/n_{\rm tot}$, hence $p_i/p_{\rm tot}$) for each species. We thus need to find the variation of $G_i$ with $p_i$, as this actually depends on the composition. At thermodynamic equilibrium[4], and constant $T$ but not constant $p_i$, we find

$$\mathrm{d}G_i = \underbrace{\delta Q_i - T\,\mathrm{d}S_i}_{0} + \underbrace{\delta W_i + p_i\,\mathrm{d}V_i}_{0} + V_i\,\mathrm{d}p_i - S_i\underbrace{\mathrm{d}T}_{0} = V_i\,\mathrm{d}p_i = n_i RT\frac{\mathrm{d}p_i}{p_i}$$

$$\Rightarrow\quad G_i(p_i) = G_i^\circ + n_i RT\ln\left(\frac{p_i}{p^\circ}\right)$$

where $G_i^\circ$ is the Gibbs free energy of species $i$ at some standard pressure $p^\circ$, usually taken to be $1\,\mathrm{atm} \approx 1\,\mathrm{bar} = 10^5\,\mathrm{Pa}$. The total Gibbs energy of the whole gas is therefore:

$$G = \sum_i G_i(p_i) = \sum_i \left[G_i^\circ + n_i RT\ln\left(\frac{p_i}{p^\circ}\right)\right] = \sum_i n_i\left[G_{m,i}^\circ + RT\ln\left(\frac{p_{\rm tot}}{p^\circ}\frac{p_i}{p_{\rm tot}}\right)\right]$$

$$\Rightarrow \frac{G}{RT} = \sum_i n_i\left[\frac{G_{m,i}^\circ}{RT} + \ln\left(\frac{n_i}{n_{\rm tot}}\right) + \ln\left(\frac{p_{\rm tot}}{p^\circ}\right)\right]$$

We must therefore minimise the above expression subject to the following constraint:

$$\sum_i a_{i\mu} n_i = b_\mu \qquad \forall\mu$$

where $b_\mu$ is the number density of element $\mu$, and $a_{i\mu}$ is the number of atoms of element $i$ in species $i$. For instance, $a_{\mathrm{CH_4,H}} = 4$. Unsurprisingly this optimisation is a task for computers.

**Example: $\mathrm{CO_2}$ and $\mathrm{CH_4}$.** In a hydrogen-rich atmosphere, an important reaction is

$$\mathrm{CO} + 3\mathrm{H_2} \rightleftharpoons \mathrm{CH_4} + \mathrm{H_2O}$$

At $p = 1\mathrm{bar}$, if $T \gtrsim 1200\mathrm{K}$, then the $G_i$ are such that the optimal composition has more CO than $\mathrm{CH_4}$; if $T \lesssim 1200\mathrm{K}$, then there is more $\mathrm{CH_4}$ than CO[5]. Jupiter and Saturn have lots of $\mathrm{CH_4}$; hot Jupiters often have lots of CO.

Composition is not just a function of $p$ and $T$, but also of elemental composition. In particular, the above equilibrium depends on the C/O ratio. Solar abundance atmospheres have an excess of oxygen: C/O = 0.5, so at low temperatures (where the C is all in $\mathrm{CH_4}$), the oxygen all goes into $\mathrm{H_2O}$. At high temperatures where CO is stable, C takes half of the O atoms into CO; with the other half remaining in $\mathrm{H_2O}$ molecules. If however, the elemental composition has C/O = 1, then at high temperatures C can take *all* of the O molecules, and there will be no $\mathrm{H_2O}$ left. $\mathrm{H_2O}$ is therefore a good *tracer* of an exoplanet's overall C/O ratio. These points are illustrated in Figure 4, stolen from Madhusudhan (2012).

Whereas $\mathrm{H_2O}$ is a good tracer of the C/O ratio, $\mathrm{CO_2}$ is a good tracer of the overall metallicity: as metallicity increases, metal-rich species like $\mathrm{CO_2}$ become much more abundant.

[4] where now $\delta Q = T\,\mathrm{d}S$

[5] Higher temperatures generally favour whichever side has more molecules. For the reaction $\mathrm{N_2} + 3\mathrm{H_2} \rightleftharpoons 2\mathrm{NH_3}$, higher temperatures ($T \gtrsim 500\mathrm{K}$) favour $\mathrm{N_2}$ over $\mathrm{NH_3}$.

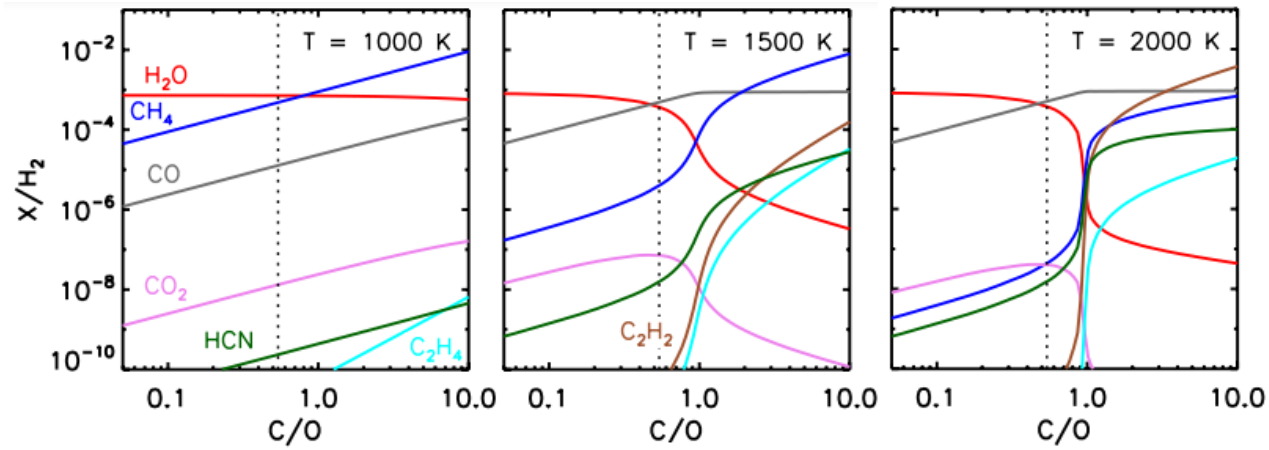


**Figure 4 | Dependence of Composition on Temperature and C/O ratio.** We see that temperatures above 1200K favour CO (grey) over $CH_4$ (blue). At low $T$ therefore, the oxygen pretty much all goes into $H_2O$. At high $T$, the amount of oxygen taken from the $H_2O$ depends on how much C there is available to form CO. With little carbon (C/O $< 1$), most of the $H_2O$ survives as there is ample O to go around. With lots of carbon (C/O $> 1$), all the oxygen is stolen into CO, with little $H_2O$ remaining.

### 2.5.2 Non-equilibrium Processes

Real exoplanetary atmospheres are not in equilibrium, with vertical mixing and photochemical processes not allowing the atmosphere to settle. Certain species can be approximated as being in equilibrium with each other if the timescale for the reaction (or, more precisely, the reaction's rate-limiting step) is significantly shorter than the timescale for non-equilibrium processes.

**Vertical Mixing.** As $p$ and $T$ vary with altitude in an atmosphere it may be that in equilibrium e.g. CO would be dominant below a certain altitude, reacting away into $CH_4$ higher up. In reality, updrafts dredge lower species up into the upper atmosphere. This explains why CO is found even in the upper atmospheres of cool planets. To tell whether this process is important, we must compare its timescale to the reaction timescale. The rate-limiting step for the CO$\rightleftharpoons$$CH_4$ equilibrium turns out to be $H_2 + CH_2OH \rightleftharpoons CH_3OH+H$, so $\tau_{\rm ch}$ is given by:

$$\frac{\mathrm{d}[\mathrm{CO}]}{\mathrm{d}t} = -k[\mathrm{H_2}][\mathrm{CH_2OH}] \qquad \Rightarrow \qquad \tau_{\rm ch} \equiv \frac{[\mathrm{CO}]}{|\mathrm{d}[\mathrm{CO}]/\mathrm{d}t|} = \frac{[\mathrm{CO}]}{k[\mathrm{H_2}][\mathrm{CH_2OH}]}$$

By comparison, the mixing timescale depends on the *Eddy diffusion coefficient* $K_{zz}$:

$$\tau_{\rm vm} \sim \frac{L^2}{K_{zz}}$$

where the length scale $L$ is approximately $0.1H_{\rm sc}$. Anyway, if $\tau_{\rm vm} \ll \tau_{\rm ch}$, then vertical mixing will dominate and the region of the atmosphere where this holds will be chemically homogeneous. This is usually the case in the upper atmosphere, where the densities of the relevant species is low and so $\tau_{\rm ch}$ is too long for chemical equilibrium to ever be achieved.

The two timescales are equal at the "quench level" $z_q$, where $p \sim 1$bar. We can thus approximate that the atmosphere above $z_q$ is roughly homogeneous. Below $z_q$, the atmosphere is roughly in chemical equilibrium, and the composition varies with height alongside $p$ and $T$.

**Photochemistry.** When $p$ dips below $\sim 10^{-3}$bar, UV/visible radiation directly interferes with the chemistry, dissociating molecules into *free radical* species (e.g. $O_2 \rightarrow 2O$) and their

by-products (e.g. $O_3$). For example, the abundances of oxygen species in the upper atmosphere are governed by the "Chapman reactions" 1–4:

$$O_2 \to 2O \qquad O + O_2 \xrightarrow{M} O_3 \qquad O_3 \to O + O_2 \qquad O + O_3 \to 2O_2$$

where reaction 2 requires a catalytic species M to carry off the energy produced; any abundant molecule will do. Each of these reactions has a *rate constant* $k_i$, such that each reaction proceeds at a rate $k_i \prod_j [X_j]$ ,where $[X_j]$ are the concentrations (number densities, perhaps) of the reactants. The rate of change of [O] and $[O_3]$ are then

$$\frac{\mathrm{d}[O]}{\mathrm{d}t} = 2k_1[O_2] - k_2[M][O][O_2] + k_3[O_3] - k_4[O][O_3]; \quad \frac{\mathrm{d}[O_3]}{\mathrm{d}t} = k_2[M][O][O_2] - k_3[O_3] - k_4[O][O_3]$$

In the steady state, both of these time derivatives will be 0, so the second equation gives:

$$[O_3] = \frac{k_2[M][O][O_2]}{k_3 + k_4[O]} \approx \frac{k_2[M][O][O_2]}{k_3}$$

where we have used the experimental fact that $k_3 \gg k_4[O]$, that is, reaction 3 is the dominant loss mechanism for $O_3$. The concentration of O is much harder to estimate than $O_2$; luckily it can be eliminated: summing the two rate equations in steady state, we find

$$0 = 2k_1[O_2] - 2k_4[O][O_3] \qquad \Rightarrow \qquad [O] = \frac{k_1[O_2]}{k_4[O_3]}$$

$$\Rightarrow [O_3] = \frac{k_2[M][O_2]}{k_3}\frac{k_1[O_2]}{k_4[O_3]} \qquad \Rightarrow \qquad [O_3] = \sqrt{\frac{k_1 k_2[M]}{k_3 k_4}}[O_2]$$

Now $[O_2]$ decreases with altitude, experimentally $k_2[M]/k_4$ is roughly constant, and $k_1/k_3$ increases with altitude. Thus there will be an altitude at which $[O_3]$ rises to a maximum concentration (due to the increasing production of O by reaction 1) before fading away (alongside every other molecule). This creates an *ozone layer*.

Many photochemical by-products have a high $\bar{\kappa}_{\mathrm{vis}}$, giving the upper atmosphere a $\gamma > 1$. As discussed above, this induces thermal inversions, such as that in the Earth's stratosphere.

**Thermal Escape.** At yet higher altitudes ($p \sim 10^{-6} - 10^{-9}$bar), particles have thermal speeds greater than the escape velocity and can leave the planet. The Maxwell distribution, proportional to $v^2 e^{-mv^2/2k_BT}$, peaks at $v_p = \sqrt{2k_BT/m}$. The temperature of atmospheric escape is for some reason taken to be such that $6v_p$ is greater than the escape velocity, $\sqrt{2GM/R}$:

$$6\sqrt{\frac{2k_BT}{m}} > \sqrt{\frac{2GM}{R}} \qquad \Rightarrow \qquad T > \frac{GMm}{36k_BR}$$

We see that this is proportional to $m$: smaller particles can escape more easily, so this process is particularly of importance in the upper atmosphere where most species are atomised by the high UV flux (rather than due to $R$, which is not much different to its surface value). For a H atom on Mars, the RHS is about 40K; for Earth, about 200K. Hence we have an atmosphere and they don't. Atmospheric escape can create a trailing cloud of atoms, leading to a dramatically asymmetric transit profile.

**Hydrodynamic Escape.** In Hot Jupiters close to stars with a high UV flux, thermal escape is rapid. The exodus of thermally escaping atoms pushes larger species (e.g. C, N, O) out with them, like adults being swept away by a crowd of running children. This may lead to *Chthonian planets*, terrestrial former gas giants whose atmospheres abandoned them.

## 2.6 Clouds & Hazes

Clouds are particles suspended in the atmosphere which have condensed out of the gas phase onto a nucleus (e.g. silicate grains). Clouds may consist of $H_2O$ (as on Earth), $NH_3$, $CH_4$ (as in Solar System gas giants) or high-temperature condensates like KCl and $SiO_2$ (*alkali/silicate clouds*). Hazes are suspended particles generated by other processes, e.g. photochemical species with high $\sigma_\lambda$, or updrafts bringing sand grains from the surface high into the atmosphere.

### 2.6.1 Scattering

Clouds and hazes have a large $\sigma_\lambda$ at optical wavelengths. There are two types of scattering:

- **Rayleigh** scattering occurs when the particle size is $\ll \lambda$: even gaseous molecules do it. It originates from the polarisability of the particle in response to the oscillating **E** field of the light. Rayleigh scattering has a characteristic $\sigma_\lambda \propto \lambda^{-4}$ for any composition.
- **Mie** scattering requires a particle size $\gtrsim \lambda$, and is the solution to Maxwell's Equations for plane waves incident on spherical particles. $\sigma_\lambda$ has no simple functional form; some species have resonances at particular $\lambda$.

### 2.6.2 Albedo

Scattering leads to reflection, which is quantified by albedo $A$. Again, there are two types:

- **Bond** albedo is simply the ratio of the reflected light (integrated over all wavelengths) to that of the incident light. Intuitive.
- **Geometric** albedo is the ratio of the reflected light observed at *full phase* (i.e. at secondary eclipse, when we can see the whole dayside) to that which would be observed from a *Lambertian disk* of the same angular size, whatever that means.

### 2.6.3 Effects on Spectra

Cloud decks completely block light from below, so effectively bring the observable "surface" of an exoplanet up into the atmosphere: rather than the planet having a radius $R$, it *appears* to have a radius $R + h_c$, where $h_c$ is the height of the cloud deck. The effect of this depends on the spectrum type, but generally leads to *muted spectral features*.

- **Emission Spectra.** It was shown in §2.2 that at high altitudes, atmospheres become isothermal. Thus if the cloud deck is high enough, the atmosphere might appear to be isothermal in its entirety. It was shown in §2.3.1 that an isothermal atmosphere has the same emission spectrum as a black body, with no spectral features, so a high cloud deck might cause the exoplanet to simply look like a black body. If the cloud deck is somewhat lower, such that $T$ does vary slightly above the clouds before settling onto an isotherm, then the slight temperature variation will lead to muted spectral features in the IR.

  In the optical, the albedo effect of clouds means that the planet is brightened.

- **Transmission Spectra.** Due to the cloud deck blocking everything from below, $\delta_\lambda = 2Rh_\lambda/R_*^2$ becomes

$$\delta_\lambda = \frac{2(R + h_c)(h_\lambda - h_c)}{R_*^2} \approx \frac{2R(h_\lambda - h_c)}{R_*^2}$$

which is smaller by a factor $(h_\lambda - h_c)/h_\lambda$. Again, clouds lead to muted spectral features.

Problematically, a species' spectral features being muted is degenerate with that species simply having a low abundance. The degeneracy may be broken by looking at the optical, where that species' abundance may be estimated from scattering signatures.

## 2.7 Atmospheric Dynamics

3D atmospheric models, known as *general circulation models*, exploit the fact that atmospheres are very thin, simplifying the Navier-Stokes equations into so-called "primitive equations". Several qualitative results of these models are presented here.

### 2.7.1 Winds

It can be shown that the acceleration due to a horizontal pressure gradient $\Delta \ln p$ is of order $R\Delta T \Delta \ln p/R$, where the ideal gas constant $R \sim 3700\text{JK}^{-1}\text{kg}^{-1}$, and $\Delta T$ is the day-night temperature contrast. The advective acceleration term in the Navier-Stokes equations is $|\mathbf{u} \cdot \boldsymbol{\nabla} \mathbf{u}| \sim u^2/R$. Setting the two equal in the steady state gives a characteristic wind speed:

$$u \sim \sqrt{R\Delta T \Delta \ln p}$$

For $\Delta T = 400\text{K}$ and $\Delta \ln p = 3$, this gives $u = 2.1\text{kms}^{-1}$. This is detectable using high-spatial-resolution Doppler spectroscopy of the transmission spectrum. Also, the phase curves of exoplanet emission spectra are often asymmetric around the secondary eclipse, suggesting that the hottest point is not the substellar point, but is offset by the winds.

### 2.7.2 Day-Night Temperature Contrast

The day-night temperature contrast on a tidally locked planet depends on the efficiency of atmospheric circulation. If it is efficient, temperature contrasts are quickly ironed out. If slow, the contrast can remain.

There's some very dodgy derivations in this section; the result is that for larger $T$, hotter planets have a much larger flux, and so radiate away heat outwards much quicker than they advect that energy around the planet. As such, hotter planets end up with a relatively cool night side (relative to the dayside), and so a larger temperature contrast.

### 2.7.3 Bands

Bands emerge due to the variation of the Coriolis force with latitude. The *Coriolis frequency* is given by $2\Omega \sin\theta$, and the latitutinal gradient of this is $\beta = 2\Omega \cos\theta/R$. The characteristic width of bands is given by the *Rhines length* $L_\beta \sim \sqrt{u/\beta} \sim \sqrt{Ru/2\Omega}$. The number of these bands that can fit onto a planet's surface is therefore

$$N_{\text{bands}} \sim \frac{R}{L_\beta} \sim \sqrt{\frac{2\Omega R}{u}}$$

For Hot Jupiters, $\Omega \approx 2\pi/1\text{day}$, $u \sim 1\text{kms}^{-1}$, so $N_{\text{bands}} \sim 1$. For Jupiter, $\Omega \approx 2\pi/0.4\text{day}$, $u \sim 40\text{kms}^{-1}$, so $N_{\text{bands}} \sim 10$. Other Solar System gas giants have smaller radii and higher wind speeds than Jupiter, so have no visible banding.

# 3 Interiors

## 3.1 Polytropes

Two equations of state governing the interior are: $\frac{\mathrm{d}m}{\mathrm{d}r} = 4\pi r^2\rho$, and $\frac{\mathrm{d}p}{\mathrm{d}r} = -\rho g = -\frac{Gm\rho}{r^2}$, where $m(r)$ is the mass contained *within* a radius $r$. Substituting $m$ from the second equation into the first, and substituting the polytropic gas equation of state $p = K\rho^{1+1/n}$, we obtain :

$$-\frac{\mathrm{d}}{\mathrm{d}r}\left(\frac{r^2}{G\rho}\frac{\mathrm{d}p}{\mathrm{d}r}\right) = 4\pi r^2\rho \qquad \Rightarrow \qquad -\frac{K}{4\pi G}\frac{n+1}{n}\frac{1}{r^2}\frac{\mathrm{d}}{\mathrm{d}r}\left(\frac{r^2}{\rho}\rho^{1/n}\frac{\mathrm{d}\rho}{\mathrm{d}r}\right) = \rho$$

Substituting $\rho(r) = \rho_c\theta(r)^n$, where the constant $\rho_c = \rho(0)$ (hence requiring $\theta(0) = 1$),

$$\underbrace{\frac{K\rho^{(1-n)/n}(n+1)}{4\pi G}}_{\alpha^2}\frac{1}{r^2}\frac{\mathrm{d}}{\mathrm{d}r}\left(r^2\frac{\mathrm{d}\theta}{\mathrm{d}r}\right) = -\theta^n \qquad \Rightarrow \qquad \boxed{\frac{1}{\xi^2}\frac{\mathrm{d}}{\mathrm{d}\xi}\left(\xi^2\frac{\mathrm{d}\theta}{\mathrm{d}\xi}\right) = -\theta^n} \qquad (\mathfrak{LE})$$

where we have defined $\alpha$ by that horrible mix of constants, and the variable $\xi = r/\alpha$. The result is the **Ł**ane-**Ɛ**mden equation, whose solutions $\theta_n(\xi)$ depend on the value of $n$. The radius $R$ is given by $R = \alpha\xi_n$, where $\xi_n$ is the first zero of $\theta_n(\xi)$, as it is here that $\rho \propto \theta_n(\xi_n)^n = 0$. For example, for $n = 1$, $\theta(\xi) = \sin\xi/\xi$, so we would have $\xi_n = \pi$ and $R = \alpha\pi$.

### 3.1.1 Mass-Radius Relations

The Lane-Emden equation can be used to give an $n$-dependent relation between $M$ and $R$:

$$M = 4\pi\int_0^R r^2\rho(r)\,\mathrm{d}r = 4\pi\rho_c\alpha^3\int_0^{\xi_n}\xi^2\theta_n(\xi)^n\mathrm{d}\xi = -4\pi\rho_c\alpha^3\int_0^{\xi_n}\frac{\mathrm{d}}{\mathrm{d}\xi}\left(\xi^2\frac{\mathrm{d}\theta}{\mathrm{d}\xi}\right)\mathrm{d}\xi$$
$$= -4\pi\rho_c\alpha^3\xi_n^2\left.\frac{\mathrm{d}\theta_n}{\mathrm{d}\xi}\right|_{\xi_n} \propto \rho_c^{1+3(1-n)/2n} = \rho_c^{(3-n)/2n}$$

whereas $R = \alpha\xi_n \propto \rho_c^{(1-n)/2n}$. Eliminating $\rho_c$, we can therefore write $R \propto M^{(1-n)/(3-n)}$.

For a constant-density sphere, we have $p$ independent of $\rho$ so $n = 0$. Hence $R \propto M^{1/3}$.

For an adiabatic monatomic gas, or a degenerate gas, $p \propto \rho^{5/3} \Rightarrow n = 3/2$, so $R \propto M^{-1/3}$; indeed this is the case deep within very large gas giants, which have either convection of a gas or degeneracy occurring within.

When plotting $R$ against $M$, models suggest that $R \propto M^{1/3}$ approximates planets quite well up to about $M_J$, at which point the relation begins to turn over to $R \propto M^{-1/3}$ by about $10M_J$; the plot peaks at about $4M_J$. At about $13M_J$, the planet becomes a brown dwarf as D fusion becomes possible. As D is only $\sim 10^{-5}$ as abundant as H, and its fusion doesn't release much energy, the brown dwarf is largely supported by electron degeneracy pressure so $R \propto M^{-1/3}$. Beyond about $70M_J$, hydrogen fusion becomes possible, the degeneracy is lifted, $n$ falls below 1 and the plot begins to rise again.

The shape of the plot is independent of composition, but for atmospheres of higher $\mu$, the radius shrinks somewhat as the atmosphere is simply heavier, requiring greater pressures.

These models tend to under-predict the radii of gas giants, for several possible reasons:

- **External energy sources.** These models do not account for external energy sources (irradiation, tidal heating etc.), which can puff up the planet.
- **Delayed contraction.** As a gas giant forms, it contracts as it cools. However, this may be delayed, e.g. by rapid inward migration, or high-$\kappa_\lambda$ species trapping heat.

# 4 Habitability

There are three requirements for life as we know it: bioessential elements (CHNOPS), an energy source (e.g. starlight) and liquid water. The latter is the least likely to occur on an exoplanet.

The habitable zone is defined as the range of distances from the star such that if Earth were placed there, liquid water would be present on the surface. The inner boundary of the Sun's habitable zone is at 0.97au. If the Earth were closer than this, the oceans would evaporate, and the stratosphere would become saturated with water, which would then photolyse into $H_2$, which would then escape. The outer boundary of the Sun's habitable zone is at 1.7au, at which point $CO_2$ would freeze out and the greenhouse effect would fail. Note that Mars is at 1.5au, within the habitable zone, but its atmosphere (or rather lack thereof) makes it unsuitable for liquid water to exist on its surface.

All else being equal, the surface temperature of a planet will be larger if it orbits a hotter star. Thus for cool stars (e.g. RDs, BDs), the habitable zone will be contracted. Around M dwarfs with $M_* \sim 0.1 M_\odot$, the HZ is around 0.1au from the star.

Habitable zones also move out over time, as stars generally brighten over their lifetimes.

Factors affecting habitability other than distance to the star may be grouped as follows:

- **Astrophysical factors.** Stellar properties and activity, orbital architecture (eccentricity, obliquity, presence of other planets), whether water can be externally delivered by e.g. comets, magnetospheric protection from the solar wind
- **Planetary conditions.** Atmospheric composition (hence greenhouse effect and UV protection), geological activity e.g. volcanism and plate tectonics (to outgas greenhouse gases like $CO_2$)

## 4.1 Biosignatures

An ideal biosignature species cannot be formed abiotically (such as geochemically or photochemically), and must be observable (have high abundance and strength of spectral features).

Candidate biosignatures are divided into primary and secondary metabolic by-products:

- **Primary:** products of processes used by life to convert environmental resources into biomass and energy. On Earth, these include:

  $$O_2, \quad H_2, \quad CO_2, \quad N_2, \quad N_2O, \quad NO, \quad NO_2, \quad H_2S, \quad CH_4, \quad H_2O$$

  Many of these are present naturally, but $O_2$ is almost uniquely biotic in origin. However, around small active stars, $O_2$ can be produced abiotically.

- **Secondary:** products not directly needed for life to survive, but for secondary benefits e.g. responses to changing conditions. On Earth, these include:

  $$OCS, \quad CS_2, \quad PH_3, \quad CH_3Cl, \quad CH_3Br, \quad (CH_3)_2S$$

  These cannot be produced abiotically, but are only present in sub-ppm concentrations on Earth. It may be possible to detect these in the atmospheres of super-Earths around M dwarfs, or on hot worlds with large $H_{\rm sc}$.

The current best bet for a good biosignature would be to find $O_2$, $N_2O$, or perhaps $CH_4$ in the atmosphere of an Earth-like planet around a Sun-like star. However, as life on other planets may be totally different to life on Earth, it will be important to keep an open mind...